A DIRECT METHOD FOR SOLVING CRACK GROWTH PROBLEMS—II. SHEAR MODE PROBLEMS

X. Li and L. M. Keer

Department of Civil Engineering, Northwestern University, Evanston, IL 60208, U.S.A.

Abstract—A direct method based on the boundary element equation approach was proposed in a previous paper (Li and Keer, 1992, Int. J. Solids Structures 29, 2735–2747) to solve tensile crack growth problems for arbitrarily distributed loads. This method is extended to solve crack growth problems under an arbitrary shear loading. An equation is derived which gives an explicit relation between the crack front variation and the resulting changes in the energy release rate. This method is then applied to determine the yield zone of cracks having an assumed shear resistance of the Dugdale type. Numerical results show a significant Poisson's ratio effect of the material on the shape of the yield zone. Averaged quantities appear quantitatively similar to results from simpler approximations.

INTRODUCTION

Three-dimensional crack growth problems are of practical interest in many engineering fields, such as hydraulic induced fracturing used in the oil industry and the analysis of damage mechanisms of structural components due to crack expansion. In contrast to stationary crack problems in which the geometry of the crack is given, the present analysis considers crack growth problems where the crack shape is not known *a priori* and must therefore be determined through the solution procedure. The procedures require that the fracture criterion be satisfied after growth for each new crack geometry.

An iteration approach has been used previously to address this class of problems. At each step the crack front advance at a point is assumed to be proportional to the difference of the stress intensity factor and the local fracture toughness of the material to a certain power. The iteration continues until an equilibrium crack front is found. One drawback of this approach is that the iteration process may not represent the actual crack growth process [see e.g. papers by Mastrojannis *et al.* (1980), Lee and Keer (1986) and Fares (1989)].

For cracks in a uniformly loaded, homogeneous medium, Rice (1985, 1987) and Gao and Rice (1986, 1987) have developed a theory for calculating the first order variation in crack face displacement and stress intensity factor due to small changes in crack geometry. The problem of finding an equilibrium crack front for the shear mode with a constant energy release rate along the front, where the crack is perturbed slightly from a circular shape, was addressed by this theory (Gao, 1988). The first order relation between the perturbation of the crack geometry and the stress intensity factor was utilized and extended to solve crack growth problems involving large crack shape deformations by Bower and Ortiz (1990).

To solve general crack growth problems without adopting an *ad hoc* crack growth law, such as is used in the iteration approach mentioned above, it is necessary to develop equations which provide an explicit relation between the crack front variation and the resulting changes in the stress intensity factor. It then becomes possible to determine the crack front advance which will result in a given variation of the stress intensity factor such that the fracture criterion is satisfied at each new crack front.

An approach was proposed by Li and Keer (1992) to derive such equations from appropriate boundary element equations, which were originally developed to solve for the crack face displacement and the stress intensity factor for stationary crack problems. It is apparent that the coefficients, as well as the solution of the boundary element equations, depend upon the shape of the crack. By considering the changes of these quantities with

respect to the positions of the points on the crack front, a perturbation type relation can be derived between the crack front displacement and the variation of the stress intensity factor. By this approach, the equations necessary to solve mode I crack growth problems are established and used, as an application, to analyse the growth of the yield zone of a Dugdale-type crack of circular shape under linear variation of load as well as of elliptical shapes under uniform load (Li and Keer, 1992).

An equation of the perturbation type, which gives an explicit relation between the crack front displacement and the resulting variation of the energy release rate related to the fracture criterion for shear mode cracks, is derived for solving the shear mode crack growth problems considered here. The approach is similar to that used for mode I crack problems, although the resulting formulae are inherently more complicated.

The equation derived is then used for the problem of determining the yield zone of penny-shaped cracks, using a Dugdale-type theory for shear loading. Such a theory might be applied when the crack is constrained to remain in a plane, such as when two identical shear-loaded half spaces are joined together by a weak bond having a penny-shaped unbonded region. Unlike the case of tensile cracks, for which analytical solutions are available for penny-shaped cracks [see, e.g. Keer and Mura (1965) and Tada et al. (1985)], the case of three-dimensional shear mode cracks have received comparatively little attention. Under the assumption that the shape of the front of the yield zone is still circular, Becker and Gross (1989) have studied this problem analytically. Their results indicate that this assumption is valid only when the Poisson's ratio of the material is much smaller than unity or when the radius of the crack face is very small compared to that of the yield zone. Since the problem is now asymmetrical, the resulting yield zone under uniform remote shear loading will inevitably deviate from a circle, which renders analysis difficult and requires the use of a numerical method, such as that proposed here.

Another difficulty associated with the shear mode crack is that the direction of the yield stress in the yield zone is also not known *a priori*. In this paper the magnitude of the yield stress is taken to be constant throughout the plastic zone while its direction is assumed to be opposite to the direction of the crack face sliding displacement and varies from point to point. Since the direction of the yield stress and the crack face displacement are mutually dependent, the problem also requires their resolution as part of the solution. It is shown that the direction of the yield stress can be determined by an iteration scheme as discussed later.

FORMULATION

Consider a planar crack in the plane $x_3 = 0$ in a full space, subjected to a shear load which induces mode II and mode III stress intensity factors around the crack front. With the crack face sliding displacements Δu^1 and Δu^2 along the x_1 and x_2 directions as the unknown functions, a system of two-dimensional singular integral equations, defined on the crack faces, has been derived by Lee *et al.* (1987), which can be written in the form:

$$\int K^{\alpha\beta}(x, x_0)\Delta u^{\beta}(x)\,dA(x) = -\tau^{\alpha}(x_0), \quad \alpha, \beta = 1, 2,$$ (1)

where τ^{α} is the shear stress along the x_α direction and $K^{\alpha\beta}(x, x_0)$ is the kernel function given as

$$K^{11}(x, x_0) = \frac{\mu}{4\pi(\kappa+1)}\left[\frac{2(\kappa-1)}{r^3} + \frac{3(3-\kappa)(x_0-x)^2}{r^5}\right],$$ (2)

$$K^{12}(x, x_0) = K^{21}(x, x_0) = \frac{\mu}{4\pi(\kappa+1)}\left[\frac{3(3-\kappa)(x_0-x)(y_0-y)}{r^5}\right],$$ (3)

$$K^{22}(x, x_0) = \frac{\mu}{4\pi(\kappa+1)} \left[\frac{2(\kappa-1)}{r^3} + \frac{3(3-\kappa)(y_0-y)^2}{r^5} \right], \tag{4}$$

where $r = \sqrt{(x_0-x)^2+(y_0-y)^2}$ and $\kappa = 3-4v$, where v is Poisson's ratio.

For a numerical solution of eqn (1) the domain of the crack face is divided into N subdomains. After putting eqn (1) into a discrete form by a proper numerical scheme (Lee et al., 1987), it is reduced to the following set of algebraic equations:

$$H_{ij}^{\alpha\beta}\Delta\bar{u}_j^{\beta} = -\tau_i^{\alpha}, \quad \alpha, \beta = 1,2, \quad i,j = 1,2,\ldots,N, \tag{5}$$

where τ_i^{α} is the shear stress in the x_α direction at the collocation point x_i:

$$H_{ij}^{\alpha\beta} = \int_{\Delta_j} K^{\alpha\beta}(x, x_i)w(x)\,dA(x).$$

Here, Δ_j is the jth subdomain (element) of the crack faces and $w(x)$ is the weight function which describes the variation of Δu within each element:

$$\Delta u(x) = \Delta\bar{u}w(x). \tag{6}$$

In this paper the weight function $w(x) = \sqrt{2a\varepsilon - \varepsilon^2}$ is adopted where ε is the shortest distance from the integration point to the crack front and a is a representative length of the crack geometry (Murakami and Nemat-Nasser, 1983).

After solving $\Delta\bar{u}$ from eqn (5) the stress intensity factor K is calculated from the crack sliding displacement of the crack front elements by the relation:

$$K_{II} = \frac{\sqrt{2\pi\mu}}{4(1-v)} \frac{\sqrt{2a\varepsilon-\varepsilon^2}}{\sqrt{\varepsilon}} (\Delta u^2\cos\theta+\Delta u^3\sin\theta), \tag{7}$$

$$K_{III} = \frac{\sqrt{2\pi\mu}}{4} \frac{\sqrt{2a\varepsilon-\varepsilon^2}}{\sqrt{\varepsilon}} (-\Delta u^2\sin\theta+\Delta u^3\cos\theta). \tag{8}$$

In turn, the energy release rate can be derived from the stress intensity factor as

$$G = \frac{1-v}{2\mu}K_{II}^2 + \frac{1}{2\mu}K_{III}^2. \tag{9}$$

In this paper the fracture criterion adopted for the shear mode crack growth is an inequality boundary condition, stating that the energy release rate has to be less than or equal to a critical value G_c, $G \leqslant G_c$, where G_c is a constant which reflects the property of the material to resist fracture.

With a continuous increase in the applied load, the value of the energy release rate will eventually reach G_c at some points along the crack front. The crack will be forced to grow by any further increment in the load. With the boundary element equation approach the crack front is defined by the positions of nodal points along the crack front. Consequently, for crack growth problems, the variation of the crack geometry during crack growth is specified by the displacements of the nodes on the crack front. In the sequel δa_j will be used to denote the displacement of the jth front node along the direction normal to the crack front. The new crack front after growth is determined by the criterion that the solution of G from eqns (5), (7), (8) and (9) for the new crack front satisfies $G \leqslant G_c$. In order to find such a crack geometry, the relation between the crack front node displacement and the resulting changes of the solution of eqn (5) has to be established. The coefficients in eqn (5) as well as the solution $\Delta\bar{u}$ apparently depend upon the shape of the crack, or the positions of the nodal points on the crack front. To study the variation in $\Delta\bar{u}$ and hence the energy

release rate caused by the crack front variation, or δa, the change of the values of quantities given in eqn (5) with respect to δa is taken as

$$H_{ij}^{\alpha\beta}\delta(\Delta\bar{u}_j^\beta) + \frac{\partial H_{ij}^{\alpha\beta}}{\partial\delta a_m}\Delta\bar{u}_j^\beta\delta a_m = -\tau_i^\alpha, \quad \alpha,\beta = 1,2, \quad i = 1,2,\ldots,N. \tag{10}$$

In the above equation the summation is given by $j = 1,\ldots,N$ and $m = 1,\ldots,M$, where M is the total number of the frontal nodes. The calculation of $\partial H_{ij}^{\alpha\beta}/\partial\delta a_m$ is similar to that discussed in the previous paper for $\partial H_{ij}/\partial\delta a_m$ (Li and Keer, 1992). The formulae for regular integrals and for Cauchy principal value integrals can be obtained from the corresponding formulae for $\partial H_{ij}/\partial\delta a_m$ by simply substituting H_{ij} with $H_{ij}^{\alpha\beta}$, which are not listed here. For the finite part integral, the formulae are given in the appendix.

The relation between the changes of $\Delta\bar{u}$ and G is derived from eqns (7), (8) and (9) as

$$\delta G = \frac{\sqrt{2\pi}}{4}\left\{\sqrt{\frac{2a\varepsilon-\varepsilon^2}{\varepsilon}}\,[\delta(\Delta u^2)(K_{II}\cos\theta - K_{III}\sin\theta) + \delta(\Delta u^3)(K_{II}\sin\theta + K_{III}\cos\theta)]\right.$$

$$\left. + \delta\left(\cos\theta\sqrt{\frac{2a\varepsilon-\varepsilon^2}{\varepsilon}}\right)(K_{II}\Delta u^2 + K_{III}\Delta u^3) + \delta\left(\sin\theta\sqrt{\frac{2a\varepsilon-\varepsilon^2}{\varepsilon}}\right)(K_{II}\Delta u^3 - K_{III}\Delta u^2)\right\}. \tag{11}$$

The equation which gives a direct relation between the crack front advance and the resulting changes in the energy release rate G can be derived from eqns (5) and (11) by performing matrix manipulation to eliminate those $\delta(\Delta\bar{u})$ of the inside elements:

$$A_{ij}\delta a_j = \delta G_i, \quad i = 1,2,\ldots,M. \tag{12}$$

In deriving eqn (12), $\delta\tau$ is taken to be zero in eqn (5). Hence δG in the above equation is produced solely by the crack advance. The variation of energy release rate caused by the variation of the load is solved from eqn (5) by letting $\delta a = 0$.

Equation (12) is solved by incorporating the fracture criterion $G \leqslant G_c$ as an inequality boundary condition on the unknowns as follows:

For crack front elements:

$$\delta G = 0, \quad \delta a \neq 0 \quad \text{if } G = G_c,$$
$$\delta G \neq 0, \quad \delta a = 0 \quad \text{if } G < G_c. \tag{13}$$

APPLICATION: ANALYSIS OF SHEAR MODE CRACKS WITH PLASTIC ZONE

For penny-shaped cracks under uniform tension applied perpendicularly to the plane of the crack, the determination of the yield zone is relatively easy, assuming that yield takes place in the plane of the crack. Since the shape of the yield zone front remains circular, an analytical approach can be employed. Under uniform remote loading conditions the resulting equation, giving the relation of the yield zone size and tensile load level, has the form (Tada et al., 1985)

$$\frac{a}{b} = \sqrt{1 - \frac{\sigma^2}{\sigma_Y^2}}, \tag{14}$$

where a and b are the radius of the crack face and the yield zone front respectively, σ is the uniform tensile stress and σ_Y is the yield stress.
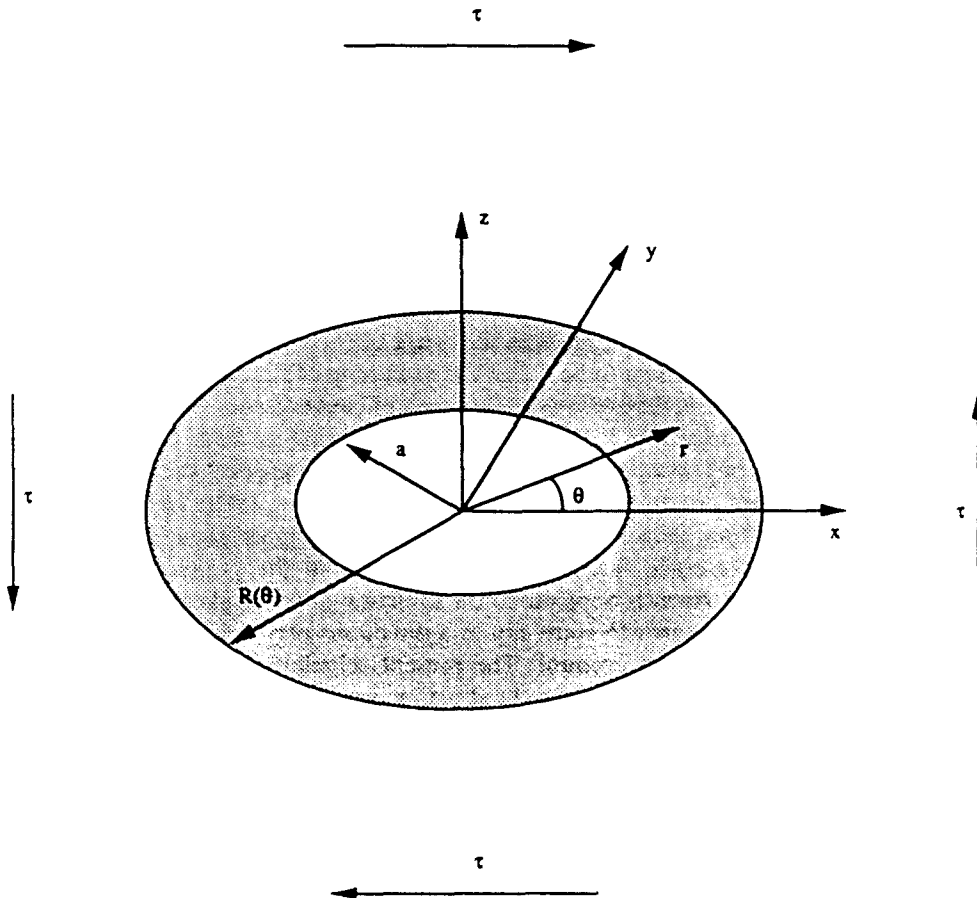
Fig. 1. Penny-shaped Dugdale crack under shear loading.

For a penny-shaped crack under uniform shear loading (Fig. 1) the shape of the yield zone front is, in general, not a circle as the load condition is now asymmetric. Becker and Gross (1989) have shown that only under the condition

$$\frac{va^2}{2b^2} \ll 1 \quad \text{and} \quad \frac{va^2}{2(1-v)b^2} \ll 1 \tag{15}$$

may the yield zone be approximated by a circular yield zone front. Under such conditions they also show that an equation similar to eqn (14) holds for shear mode cracks. It is observed that the conditions in eqn (15) are satisfied only when the Poisson's ratio, $v \ll 1$ or when the yield zone is much larger than the crack dimension, which is not the case for most applications.

In the sequel the method described in the preceding section is used to investigate the shape and size of the yield zone of penny-shaped cracks under uniform shear loading. The geometry and the loading are as shown in Fig. 1. The radius, a, of the penny-shaped crack is taken to be unity and the direction of the uniform remote shear load τ is along the x-axis. The load in the yield zone $a < r < R(\theta)$ is the sum of the remote shear load τ and the yield shear stress with constant magnitude τ_Y. The direction of the yield stress is taken in the opposite direction of the crack face sliding displacement, whose direction varies from point to point and in general deviates from the direction of the applied shear τ when Poisson's ratio is not zero. To solve this problem, which is highly nonlinear, an iterative scheme described below is used.

Let the direction vector of the crack face sliding displacement and the yield stress in the ith iteration step be $(n_x^{(i)}, n_y^{(i)})$ and $(\tau_x^{(i)}, \tau_y^{(i)})$, respectively. At the beginning of the iteration

the direction of the yield stress is assumed to be opposite to the direction of the shear loading: $(\tau_x^{(0)}, \tau_y^{(0)}) = (-1, 0)$. The crack face displacement is solved from eqn (5) and its direction $(n_x^{(0)}, n_y^{(0)})$ at each point is calculated. The direction of the yield stress of the ith step is calculated from the results of the previous step by

$$\tau_x^{(i)} = \tau_x^{(i-1)} - \lambda(n_x^{(i)} + \tau_x^{(i-1)}),$$

$$\tau_y^{(i)} = \sqrt{1 - (\tau_x^{(i)})^2}, \tag{16}$$

where $\lambda < 1$ is a multiplier. The corresponding $(n_x^{(i)}, n_y^{(i)})$ are obtained by solving eqn (5). The iteration continues until the average value of the inner product $n^{(i)} \cdot \tau^{(i)} = n_x^{(i)} \tau_x^{(i)} + n_y^{(i)} \tau_y^{(i)}$ in the yield zone is in the range of $(-0.9999, -1.0)$. In the present calculation the value of λ is taken to be 0.2 at the beginning of the iteration, which can be adjusted during the iteration, depending on the speed of convergence.

Some previous investigations in order to simplify the analysis have assumed that the direction of the yield stress is opposite to the direction of the applied shear stress (along the x-axis in the configuration shown in Fig. 1), (Becker and Gross, 1989). In our calculation when Poisson's ratio is not zero it is observed that a given applied shear stress in the x-direction will result in a crack face sliding displacement in the y-direction. Thus, the assumption that the yield stress is opposite to the direction of the applied shear will fail to reproduce the correct crack growth since slip in a directions perpendicular to the applied load is not correctly taken into account. The present calculation does assume that the direction of the yield stress corresponds to the slip direction. Although the error for a single calculation may not be too large, the accumulated error may be large when growth is considered.

The criterion used here to determine the yield zone front is that G, the energy release rate, should be equal to zero at the yield zone front and is equivalent to requiring that the stress singularity vanish. For a given remote shear load, the perturbation starts from an initial circular yield zone front $R(\theta) = C$. Equation (5) is solved and a value of $G \neq 0$, is calculated that varies along the front with the maximum and minimum values at $\theta = 0$ and $\theta = \pi/2$ respectively. Equation (12) is used to determine the crack front displacement δa, which will reduce the energy release rate along the front. The change of energy release rate δG in eqn (12) is specified as $-\alpha G_i$. To ensure accuracy the value of α is chosen such that the maximum node displacement is less than 0.01, and the analysis is repeated for the perturbed new front. The perturbation continues until G along the yielding zone front is approximately zero, considering the error associated with the solution of the original boundary element eqn (5). In the present computation $G < 0.0002$ is considered to be sufficiently small to be taken as zero. At this stage the actual yield zone front is considered to have been found.

The computation is carried out for two different values of Poisson's ratio: $v = 0.2$ and $v = 0.4$ and for various shear load levels. The numerical results are presented in Figs 2-8. In Figs 2 and 3, where because of the symmetry of the problem only the upper half of the crack geometry is shown, the thicker solid line represents the penny-shaped crack front while the other curves give the yield zone fronts corresponding to various shear loading levels ranging from $0.25\tau_y$ to $0.85\tau_y$ with increment $0.1\tau_y$.

Figures 4 and 5 give a closer look at the variation of the width of the yield zone along the crack front. The eight curves from lowest to the uppermost in each figure represent the yield zone widths corresponding to a shear load of increasing magnitudes from $0.25\tau_y$ to $0.95\tau_y$ with increment $0.1\tau_y$. It is clear from Figs 4 and 5 that the difference between the widths of the yield zone at $\theta = 0$ and $\theta = \pi/2$ increases with the increase in the shear loading level.

To measure the deviation of the shape of the yield zone front from a circle, the size of the yield zone must be taken into account. Here the quantity

$$\gamma = (\text{width} - \text{average width})/\text{average width} \tag{17}$$

is used to measure the comparative deviation of the yield zone front from a circle. When the yield zone front is a circle, γ equals zero.
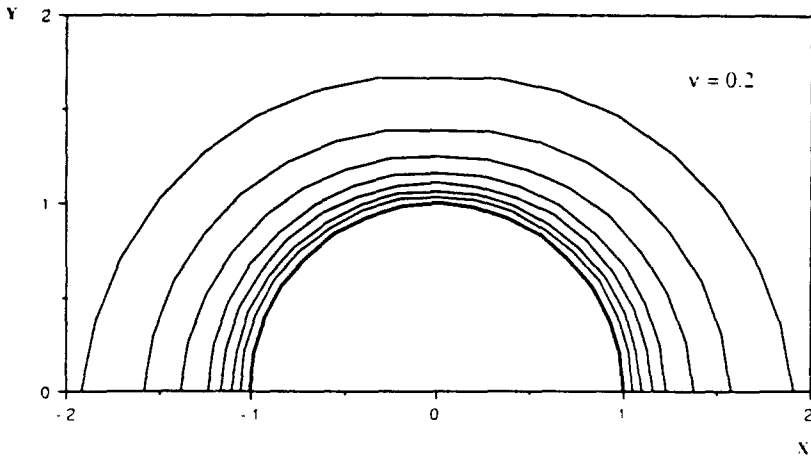
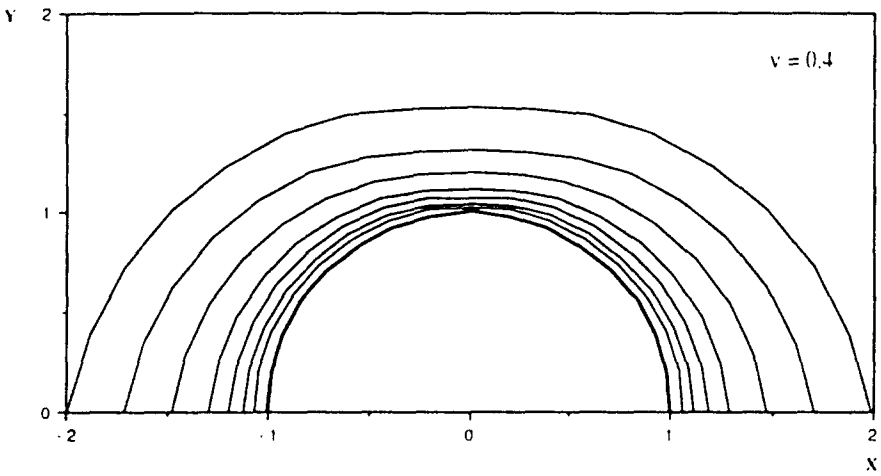Fig. 2. Yielding zones corresponding to various load levels.

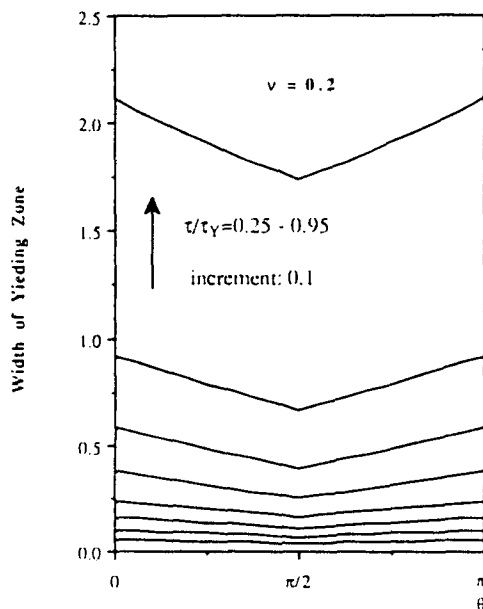Fig. 3. Yielding zones corresponding to various load levels.

Fig. 4. Variation of the width of yielding zone along the crack front.
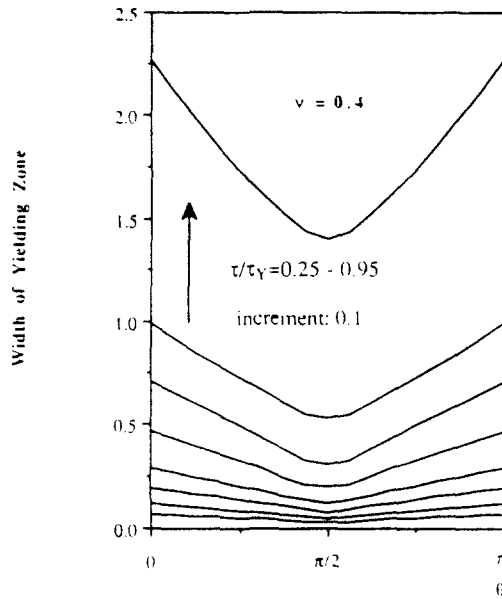
Fig. 5. Variation of the width of yielding zone along the crack front.

The results are shown in Figs 6 and 7. It is noted that in the load range from $0.25\tau_y$ to $0.65\tau_y$ the corresponding curves are nearly indistinguishable from each other, which implies that in this range of load level the yield zone grows while its shape remains almost unchanged. It is noted that the deviation of the shape of the yield zone front from a circle begins to decrease only after the magnitude of the shear load reaches a comparatively high level.

Equation (15) (Becker and Gross, 1989) implies that when b, the radius of the yield zone front, is much larger than a, a circular yield front meets the vanishing stress singularity criterion. The results here (Figs 6 and 7) show that when the yield zone grows, it will gradually approach a circle only in the sense of eqn (17). The absolute difference between the width at a point and the average width may actually increase as can be seen from Figs 4 and 5.
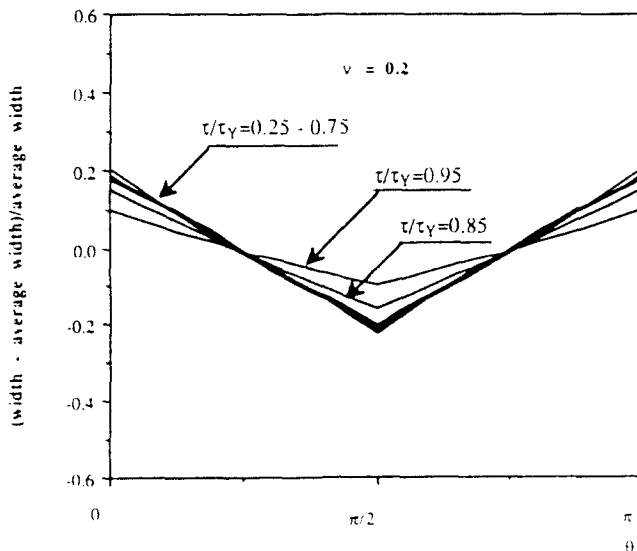

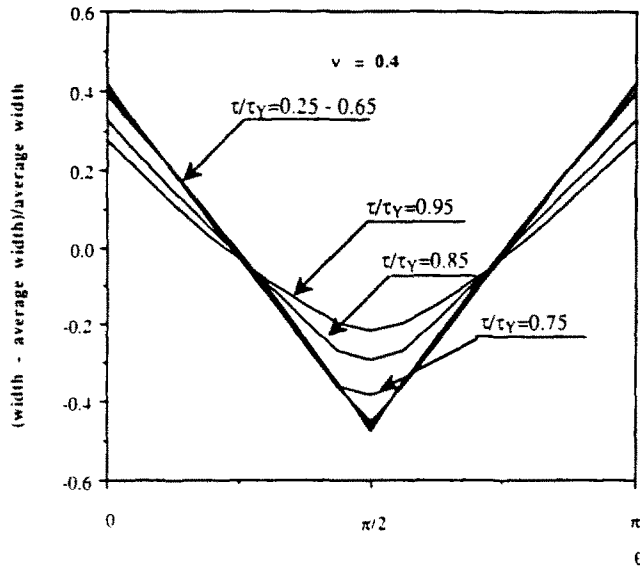Fig. 6. Deviation of yielding zone front from a circle.

Fig. 7. Deviation of yielding zone front from a circle.

The value of the Poisson's ratio of a material has a profound effect on the shape of the yield zone as can be seen by comparing Figs 4 and 5, as well as Figs 6 and 7. It is observed that when v is increased from 0.2 to 0.4, the maximum deviation of the yield zone width from the average value is nearly doubled.

Becker and Gross (1989) have shown that for cracks using a Dugdale-type approximation under uniform shear loading, for the conditions of eqn (15) the yielding zone front can be approximated by a circle and the following equation, similar to eqn (14), holds:

$$a/b = (1 - \tau^2/\tau_Y^2)^{1/2}. \tag{18}$$

The numerical results here (Fig. 8) indicate that eqn (18) gives a good estimation of the average width of the yield zone for different values of Poisson's ratio, although the pointwise estimate is not accurate.
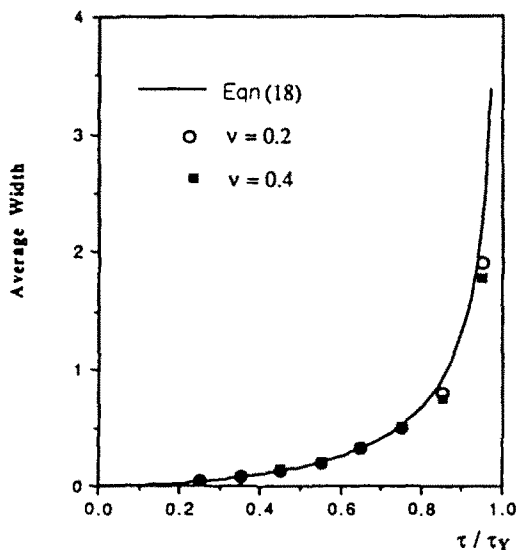

Fig. 8. Variation of average width vs load level.

REFERENCES

Becker, W. and Gross, D. (1989). About the penny-shaped Dugdale crack under shear and triaxial loading. ICF7, pp. 2289–2299.

Bower, A. F. and Ortiz, M. (1990). Solution of crack problems by a finite perturbation method. *J. Mech. Phys. Solids* **38**, 443–480.

Fares, N. (1989). Crack front trapped by arrays of obstacles: Numerical solutions based on surface integral representation. *J. Appl. Mech.* **56**, 837–843.

Gao, H. (1988). Nearly circular shear mode cracks. *Int. J. Solids Structures* **24**, 177–193.

Gao, H. and Rice, J. R. (1986). Shear stress intensity factors for a planar crack with slightly curved front. *J. Appl. Mech.* **53**, 774–778.

Gao, H. and Rice, J. R. (1987). Somewhat circular tensile cracks. *Int. J. Frac.* **33**, 155–174.

Keer, L. M. and Mura, T. (1965). Stationary crack and continuous distributions of dislocations. *Proc. First Int. Conf. on Fracture*, Vol. 1, pp. 99–115 (Edited by T. Yokobori, T. Kawasaki and J. L. Swedlow). Published under the auspices of The Unified Research Society for Micro and Macro Behaviour of Materials and the Japan Society for the Promotion of Science.

Lee, J. C., Farris, T. N. and Keer, L. M. (1987). Stress intensity factors for cracks of arbitrary shape near an interfacial boundary. *Engng Fract. Mech.* **27**, 27–41.

Lee, J. C. and Keer, L. M. (1986). Study of a three-dimensional crack terminating at an interface. *J. Appl. Mech.* **53**, 311–316.

Li, X. and Keer, L. M. (1992). A direct method for solving crack growth problems—I. *Int. J. Solids Structures* **29**, 2735–2747.

Lin, W. and Keer, L. M. (1987). Scattering by a planar three-dimensional crack. *J. Acoust. Soc. Am.* **82**, 1442–1448.

Mastrojannis, L. M., Keer, L. M. and Mura, T. (1980). Growth of planar cracks induced by hydraulic fracturing. *Int. J. Numer. Meth. Engng* **15**, 41–54.

Murakami, Y. and Nemat-Nasser, S. (1983). Growth and stability of interacting surface flaws of arbitrary shape. *Engng Fract. Mech.* **17**, 193–210.

Rice, J. R. (1985). First order variation in elastic fields due to variation in location of a planar crack front. *J. Appl. Mech.* **52**, 571–579.

Rice, J. R. (1987). Weight function theory for three-dimensional elastic crack analysis. In *Fracture Mechanics: Perspectives and Directions*, Twentieth Symposium (Edited by R. P. Wei and R. P. Gangloff) pp. 29–57, ASTM-STP-1020, American Society for Testing and Materials, Philadelphia.

Tada, H., Parris, P. C. and Irwin, G. R. (1985). *The Stress Analysis of Cracks Handbook* (2nd edn). Paris Production, St Louis.

APPENDIX

In the appendix formulae are given to calculate the derivatives of the finite part integral with respect to the positions of the collocation point and the nodal points. By inspecting eqns (2)–(4), it appears that the finite part integral can be calculated as the sum of two integrals:

$$I_1 = \text{F.P.} \int \frac{1}{R} \, dA \tag{A1}$$

and

$$I_{ij} = \text{F.P.} \int \frac{\tilde{x}_i \tilde{x}_j}{R^3} \, dA, \tag{A2}$$

where the integration is over the triangular element of node x_1, x_2 and x_3 with a collocation point at x_0; $\tilde{x}_i = x_0 - x$, $\tilde{x}_j = y_0 - y$. In order to derive a closed form expression of the finite integral, a local (η, ξ) coordinate with the origin at x_0 and the η axis parallel to $x_1 x_2$ is chosen. The local coordinate (η_i, ξ_i) of the ith node is related to the global coordinate (x_i, y_i) through

$$\eta_i = (x_i - x_0) \cos\theta + (y_i - y_0) \sin\theta, \tag{A3}$$

$$\xi_i = -(x_i - x_0) \sin\theta + (y_i - y_0) \cos\theta, \tag{A4}$$

where

$$\sin\theta = \frac{y_2 - y_1}{\sqrt{(x_2 - x_1)^2 + (y_2 - y_1)^2}}, \tag{A5}$$

$$\cos\theta = \frac{x_2 - x_1}{\sqrt{(x_2 - x_1)^2 + (y_2 - y_1)^2}}. \tag{A6}$$

Lin and Keer (1987) have shown that

$$I_3 = \frac{1}{\xi_3}\left(\frac{\gamma_{03}}{\beta_1} - \frac{\gamma_{01}}{\beta_2}\right) - \frac{1}{\xi_1}\left(\frac{\gamma_{01}}{\beta_1} - \frac{\gamma_{02}}{\beta_2}\right). \tag{A7}$$

$$I_2 = \frac{1}{\gamma_{03}}\left(\frac{\eta_1}{\beta_2} - \frac{\eta_3}{\beta_1}\right) - \left(\frac{\eta_2}{\beta_2\gamma_{02}} - \frac{\eta_1}{\beta_1\gamma_{01}}\right). \tag{A8}$$

$$I_4 = \frac{1}{\gamma_{03}}\left(\frac{\xi_3}{\beta_2} - \frac{\xi_3}{\beta_1}\right) - \left(\frac{\xi_2}{\beta_2\gamma_{02}} - \frac{\xi_1}{\beta_1\gamma_{01}}\right). \tag{A9}$$

$$I_{ij} = [a(2I_3 + I_4) + bI_2 + c(I_3 - I_4)]\,3. \tag{A10}$$

where

$$\gamma_{0i} = |x_0 - x_i|, \quad \beta_i = \eta_i - \xi_1(\eta_3 - \eta_1)\,(\xi_3 - \xi_i)$$

and

$$a = \sin^2\theta, \quad b = -2\cos\theta\sin\theta, \quad c = \cos^2\theta, \quad \text{for } I_{11},$$
$$a = \cos^2\theta, \quad b = 2\cos\theta\sin\theta, \quad c = \sin^2\theta, \quad \text{for } I_{22},$$
$$a = -\cos\theta\sin\theta, \quad b = \cos^2\theta - \sin^2\theta, \quad c = -a, \quad \text{for } I_{12} \text{ and } I_{21}.$$

It is apparent that the calculation of the derivatives of I_{ij} is straightforward if the derivatives of I_2, I_3 and I_4 are given. The derivatives of I with respect to x_0, x_1, x_2 and x_3 have the form:

$$\frac{\partial I}{\partial x_i} = \sum_{j=1}^{3}\left(\frac{\partial I}{\partial \xi_j}\frac{\partial \xi_j}{\partial x_i} + \frac{\partial I}{\partial \eta_j}\frac{\partial \eta_j}{\partial x_i}\right). \tag{A11}$$

$$\frac{\partial I}{\partial y_i} = \sum_{j=1}^{3}\left(\frac{\partial I}{\partial \xi_j}\frac{\partial \xi_j}{\partial y_i} + \frac{\partial I}{\partial \eta_j}\frac{\partial \eta_j}{\partial y_i}\right). \tag{A12}$$

In the above equations

$$\frac{\partial \xi_j}{\partial x_i}, \frac{\partial \xi_j}{\partial y_i}, \frac{\partial \eta_j}{\partial x_i} \quad \text{and} \quad \frac{\partial \eta_j}{\partial y_i}$$

are calculated from (A3)–(A6).

$$\frac{\partial I_3}{\partial \xi_j} \quad \text{and} \quad \frac{\partial I_3}{\partial \eta_j}$$

are given in our previous paper (Li and Keer, 1992) whereas the rest of the necessary formulae are presented below:

$$\frac{\partial I_2}{\partial \xi_1} = -\frac{1}{\beta_1^2}\left(\frac{\eta_3}{\gamma_{03}} - \frac{\eta_1}{\gamma_{01}}\right)\frac{\xi_1(\eta_3 - \eta_1)}{(\xi_3 - \xi_1)^2} - \frac{\xi_1}{\beta_1}\frac{\eta_1}{\gamma_{01}}. \tag{A13}$$

$$\frac{\partial I_2}{\partial \xi_2} = -\frac{1}{\beta_2^2}\left(-\frac{\eta_3}{\gamma_{03}} + \frac{\eta_2}{\gamma_{02}}\right)\frac{\xi_1(\eta_3 - \eta_2)}{(\xi_3 - \xi_2)^2} + \frac{\xi_2}{\beta_2}\frac{\eta_2}{\gamma_{02}}. \tag{A14}$$

$$\frac{\partial I_2}{\partial \xi_3} = \frac{\xi_3\eta_3}{\gamma_{03}}\left(\frac{1}{\beta_1} - \frac{1}{\beta_2}\right) - \frac{1}{\beta_2^2}\left(\frac{\eta_3}{\gamma_{03}} - \frac{\eta_2}{\gamma_{02}}\right)\frac{\xi_2(\eta_3 - \eta_2)}{(\xi_3 - \xi_2)^2} - \frac{1}{\beta_1^2}\left(-\frac{\eta_3}{\gamma_{03}} + \frac{\eta_1}{\gamma_{01}}\right)\frac{\xi_1(\eta_3 - \eta_1)}{(\xi_3 - \xi_1)^2}. \tag{A15}$$

$$\frac{\partial I_2}{\partial \eta_1} = \frac{1}{\beta_1^2}\left(\frac{\eta_3}{\gamma_{03}} - \frac{\eta_1}{\gamma_{01}}\right)\frac{\xi_1}{(\xi_3 - \xi_1)} + \frac{1}{\gamma_{01}\beta_1} - \frac{\eta_1^2}{\beta_1\gamma_{01}}. \tag{A16}$$

$$\frac{\partial I_2}{\partial \eta_2} = \frac{1}{\beta_2^2}\left(-\frac{\eta_3}{\gamma_{03}} + \frac{\eta_2}{\gamma_{02}}\right)\frac{\xi_1}{(\xi_3 - \xi_2)} - \frac{1}{\gamma_{02}\beta_2} + \frac{\eta_2^2}{\beta_2\gamma_{02}}. \tag{A17}$$

$$\frac{\partial I_2}{\partial \eta_3} = \frac{1}{\beta_2^2}\left(\frac{\eta_3}{\gamma_{03}} - \frac{\eta_2}{\gamma_{02}}\right)\frac{\xi_2}{(\xi_3 - \xi_2)} + \frac{1}{\beta_1^2}\left(-\frac{\eta_3}{\gamma_{03}} + \frac{\eta_1}{\gamma_{01}}\right)\frac{\xi_1}{(\xi_3 - \xi_1)} + \frac{\eta_3^2}{\gamma_{03}}\left(\frac{1}{\beta_1} - \frac{1}{\beta_2}\right) - \frac{1}{\gamma_{03}}\left(\frac{1}{\beta_1} - \frac{1}{\beta_2}\right). \tag{A18}$$

$$\frac{\partial I_4}{\partial \xi_1} = \frac{1}{\beta_1^2}\left(-\frac{\xi_3}{\gamma_{03}} + \frac{\xi_1}{\gamma_{01}}\right)\frac{\xi_1(\eta_3 - \eta_1)}{(\xi_3 - \xi_1)^2} - \frac{\xi_1^2}{\beta_1\gamma_{01}} + \frac{1}{\beta_1\gamma_{01}}. \tag{A19}$$

$$\frac{\partial I_4}{\partial \xi_2} = \frac{1}{\beta_2^2}\left(\frac{\xi_3}{\gamma_{03}} - \frac{\xi_2}{\gamma_{02}}\right)\frac{\xi_1(\eta_3 - \eta_2)}{(\xi_3 - \xi_2)^2} + \frac{\xi_2^2}{\beta_2\gamma_{02}} - \frac{1}{\beta_2\gamma_{02}}. \tag{A20}$$

$$\frac{\partial I_4}{\partial \xi_1} = -\frac{1}{\beta_2^2}\left(\frac{\xi_1}{\gamma_{01}} - \frac{\xi_2}{\gamma_{02}}\right)\frac{\xi_2(\eta_1 - \eta_2)}{(\xi_1 - \xi_2)^2} - \frac{1}{\beta_1^2}\left(-\frac{\xi_1}{\gamma_{01}} + \frac{\xi_1}{\gamma_{01}}\right)\frac{\xi_1(\eta_1 - \eta_1)}{(\xi_1 - \xi_1)^2} - \left(\frac{1}{\beta_1} - \frac{1}{\beta_2}\right)\left(\frac{1}{\gamma_{01}} - \frac{\xi_1^2}{\gamma_{01}}\right). \qquad (A21)$$

$$\frac{\partial I_4}{\partial \eta_1} = \frac{1}{\beta_1^2}\left(\frac{\xi_1}{\gamma_{01}} - \frac{\xi_1}{\gamma_{01}}\right)\frac{\xi_1}{(\xi_1 - \xi_1)} - \frac{\xi_1 \eta_1}{\beta_1 \gamma_{01}^3}, \qquad (A22)$$

$$\frac{\partial I_4}{\partial \eta_2} = -\frac{1}{\beta_2^2}\left(\frac{\xi_1}{\gamma_{01}} - \frac{\xi_2}{\gamma_{02}}\right)\frac{\xi_1}{(\xi_1 - \xi_2)} + \frac{\xi_2 \eta_2}{\beta_2 \gamma_{02}^3}, \qquad (A23)$$

$$\frac{\partial I_4}{\partial \eta_1} = \frac{1}{\beta_2^2}\left(\frac{\xi_1}{\gamma_{01}} - \frac{\xi_2}{\gamma_{02}}\right)\frac{\xi_2}{(\xi_1 - \xi_2)} - \frac{1}{\beta_1^2}\left(\frac{\xi_1}{\gamma_{01}} - \frac{\xi_1}{\gamma_{01}}\right)\frac{\xi_1}{(\xi_1 - \xi_1)} + \left(\frac{1}{\beta_1} - \frac{1}{\beta_2}\right)\frac{\xi_1 \eta_1}{\gamma_{01}^3}. \qquad (A24)$$